

Geophysical Research Letters®



RESEARCH LETTER

10.1029/2021GL097452

Key Points:

- The primary streamers of fast breakdown in Narrow Bipolar Events trigger a secondary fast breakdown of the opposite polarity
- Secondary fast breakdown is analyzed by using a new proposed model
- The current pulse of Narrow Bipolar Events is not extinguished at the end of the discharge but instead reverses its direction

Supporting Information:

Supporting Information may be found in the online version of this article.

Correspondence to:

D. Li and A. Luque,
dsl@iaa.es;
aluque@iaa.es

Citation:

Li, D., Luque, A., Gordillo-Vázquez, F. J., Silva, C. d., Krehbiel, P. R., Rachidi, F., & Rubinstein, M. (2022). Secondary fast breakdown in narrow bipolar events. *Geophysical Research Letters*, 49, e2021GL097452. <https://doi.org/10.1029/2021GL097452>

Received 14 DEC 2021

Accepted 24 MAR 2022

Secondary Fast Breakdown in Narrow Bipolar Events

Dongshuai Li¹ , Alejandro Luque¹ , F. J. Gordillo-Vázquez¹ , Caitano da Silva², Paul R. Krehbiel² , Farhad Rachidi³ , and Marcos Rubinstein⁴ 

¹Instituto de Astrofísica de Andalucía (IAA), CSIC, Granada, Spain, ²Langmuir Laboratory for Atmospheric Research, New Mexico Institute of Mining and Technology, Socorro, NM, USA, ³Electromagnetic Compatibility Laboratory, Swiss Federal Institute of Technology (EPFL), Lausanne, Switzerland, ⁴University of Applied Sciences and Arts Western Switzerland, Yverdon-les-Bains, Switzerland

Abstract The physical mechanism of Narrow bipolar events (NBEs) has been studied for decades but it still holds many mysteries. Recent observations indicate that the fast breakdown discharges that produce NBEs sometimes contain a secondary fast breakdown that propagates back in the opposite direction but this has not been fully addressed so far in electromagnetic models. In this study, we investigate fast breakdown using different approaches that employ a Modified Transmission Line with Exponential decay (MTLE) model and propose a new model, named “rebounding MTLE model,” which reproduces the secondary fast breakdown current in NBEs. The model provides new insights into the physics of the fast breakdown mechanism.

Plain Language Summary Narrow bipolar events (NBEs) are intense, bipolar-shaped radio signals emitted from thunderstorms. Because their origin is still poorly understood, they have attracted a great deal of interest in the atmospheric electricity community. Recently, it has been found that NBEs are likely produced by extensive electrical discharges named fast breakdown which are likely composed of millions of thin filaments called streamers. In this study, we propose a model for the fast breakdown current in which we consider that the primary streamer discharge triggers a second breakdown wave, also composed of streamers and propagating in the opposite direction. Our model unveils features of the fast breakdown that can play a key role in our understanding of this phenomenon.

1. Introduction

Narrow bipolar events (NBEs), sometimes also known as narrow bipolar pulses (NBPs), are impulsive and powerful radio emissions from intracloud discharges characterized by intense very high frequency (VHF) radiation, fast propagation speed and short-duration bipolar spheric waveforms in the Low Frequency band (Smith et al., 1999, 2002, 2004). NBEs have received great attention since first discovered in the 1980s (Le Vine, 1980; Willett et al., 1989) but their physical mechanism, possibly related to how lightning is initiated inside thunderstorms, remains poorly understood.

Over the past decades, several physical mechanisms have been put forward to describe NBEs. One proposal argued that NBEs are caused by energetic particles from cosmic ray air showers triggering relativistic runaway electron avalanches (RREA), a model known as the relativistic runaway electron avalanches-extensive air showers (RREA-EAS) model or as the Runaway Breakdown (RB)-EAS model (e.g., Gurevich et al., 1999; Gurevich & Zybin, 2001). Other explanations require or suggest the presence of leaders before the NBE source current (Da Silva & Pasko, 2015; Karunarathne et al., 2016).

These models are challenged by the latest observations enabled by broadband digital interferometry of lightning (Stock et al., 2014). By combining an interferometer (INTF) with a fast antenna (FA) and a lightning mapping array (LMA), Rison et al. (2016) found that positive-polarity NBEs are associated with a new type of discharge which they named fast positive breakdown (FPB), with features incompatible either with the RREA-EAS model or the existence of highly conducting channels. Tilles et al. (2019) extended these observations to negative-polarity NBE, which they found to be similarly caused by Fast Negative Breakdown (FNB). Lyu et al. (2019) found NBEs to initiate some but far from the majority of lightning discharges, the remaining fraction being initiated by an unknown process emitting weak, extremely short VHF pulses, named initial events (IEs) or the electromagnetic activities before the initial breakdown pulses (IBPs) by some authors (e.g., Karunarathne et al., 2014; Kostinskiy et al., 2020; Marshall et al., 2019, 2014). It is interesting to note that both the IEs and the fast breakdowns of

© 2022 The Authors.

This is an open access article under the terms of the [Creative Commons Attribution-NonCommercial License](https://creativecommons.org/licenses/by/4.0/), which permits use, distribution and reproduction in any medium, provided the original work is properly cited and is not used for commercial purposes.

the initiation-type NBEs (INBEs; Wu et al., 2014) or weak/less-strong NBEs (Rison et al., 2016) can potentially produce an ionized path to further initiate a stepped leader (Karunarathne et al., 2014; Stolzenburg et al., 2013).

As a consequence of these observations, it is generally accepted that Fast Breakdown (FB, encompassing both FPB and FNB) is the source of all NBEs and that it involves the propagation of a system of streamers (Attanasio et al., 2019; Cooray et al., 2020; Griffiths & Phelps, 1976; Luque & Ebert, 2014; Phelps, 1974). These streamers, possibly initiated by ice hydrometeors (Petersen et al., 2006, 2015), propagate hundreds of meters at a speed of a few times 10^7 m/s (although recently [Liu et al., 2021] pointed out that the observations are also compatible with a series of streamer bursts at fixed locations) and intensify the electric field in the starting region. Besides the observations listed above, additional studies also support this conclusion, including the analysis of radio spectra (Liu et al., 2019) and space-based optical observations (Li et al., 2021; Soler et al., 2020).

Some observations show that NBE-producing fast breakdowns sometimes contain a secondary fast breakdown that propagates in the opposite direction along the previous path (Attanasio et al., 2021; Rison et al., 2016; Tilles et al., 2019). Hamlin et al. (2007) discussed secondary pulses in the NBE signatures and interpreted them as a signature of reflection off the far end of the channel. Leal et al. (2019) examined more than 1000 NBE waveforms and found a majority of them exhibiting secondary peaks and oscillations, suggesting that these structures are a fundamental property of NBE waveforms.

Recently, Tilles et al. (2020) found alternating-polarity streamer fronts associated to energetic in-cloud pulses (EIPs). Huang et al. (2021) also found fast breakdown events consisting of simultaneous upward and downward streamer fronts, with the trajectory of the later streamer development pointing back to the initial source location. Most recently, Attanasio et al. (2021) discussed the physical mechanism of this secondary fast breakdown of NBEs based on an improved version of the Griffiths and Phelps model (Griffiths & Phelps, 1976).

Simplifying the NBE source as an infinitesimally short dipole (Nag & Rakov, 2010a; Smith et al., 1999, 2004) or as a more complex Transmission Line (Smith et al., 1999, 2004; Watson & Marshall, 2007; Nag & Rakov, 2010a,b), allows inferring properties of the source current from ground-based electromagnetic measurements. Using a TL representation of NBEs, Nag and Rakov (2010a) proposed a bouncing-wave model, where a current pulse travels consecutively and repeatedly upward and downward. As discussed later, a TL representation of the current pulse can, with appropriate modifications, explain the existing electromagnetic observations. Often TL models suppose the existence of a conducting channel but, given the evidence provided by Rison et al. (2016), where no activity is observed before the initiation of the main current pulse, it seems unlikely that a conducting channel is established before the NBE current source. In addition, the recent space-based optical observations by Soler et al. (2020); Li et al. (2021) indicate that hot channels are absent during isolated NBEs (Kostinskiy et al., 2020; Rison et al., 2016) emissions. However, the physical mechanism of fast breakdowns of the initial type NBEs (Rison et al., 2016; Wu et al., 2014) remains poorly understood. Stolzenburg et al. (2021) analyzed five IC flashes and in four of them reported faint light emissions ($\leq 5\%$ above background cumulative intensity) at the time of the IEs. Recently López et al. (2022) investigated the initiation of four lightning flashes detected from LMA and simultaneous optical satellite observations and found that, in three of the flashes, the detection of blue emissions without any red luminosity supports the pure streamer nature of fast breakdown processes at the flash initiation. However, the onset of the fourth flash was associated with both blue and red radiation and accompanied by an NBE with weak VHF power.

In their work, Rison et al. (2016) also applied a TL model to explain their FA observations and inferred a current profile that matched the observations without reflected current pulses. However, as we discuss below, this agreement resulted from the use of Shao's equation (Shao et al., 2004, 2005) for the electromagnetic radiation field. The validity of Shao's equation rests on the assumption that the current pulse has decayed completely as it reaches the endpoint of the discharge. The equation works well for a return stroke since its channel is typically long enough to justify this assumption (Shao et al., 2012), but it remains unclear whether this condition can be safely assumed in the current profile inferred by Rison et al. (2016).

In this letter, we re-analyze the data presented by Rison et al. (2016). We compute, without Shao's approximation, the electromagnetic emissions from the current profile proposed by Rison et al. (2016) and show that they exhibit a radiation peak that is missing in the observed sferic. This raises the question of why Shao's expression works better than the full Maxwell equations in fitting the data. We show below that this has a physical explanation and unveils a secondary, counter-propagating current pulse, which is consistent with the recently reported secondary

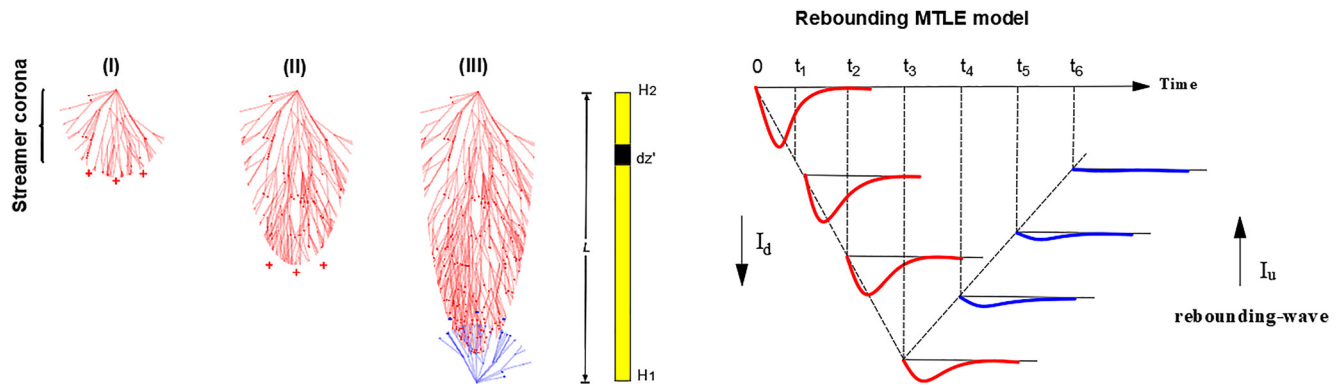


Figure 1. The rebounding MTLE model of streamer-based NBEs, (I)–(III) are different growth stages of the streamer corona system of NBEs. We model the NBE discharge channel as a system of positive streamer coronas that propagate downward from an altitude H_2 to H_1 with a channel length L , followed by upward negative streamer corona discharges that propagate back along the same path. Here, I_d is the downward current and I_u is the rebounding-wave current.

fast breakdown of NBEs. We propose a new model called rebounding Modified Transmission Line with Exponential decay (MTLE) model, to explain the secondary fast breakdown current in NBEs which is likely driven by counter-propagating streamers triggered by the primary fast breakdown pulse. The existence of this secondary streamer wave, suggesting that the fast breakdown does not completely dissipate its driving electric field, is a new key to our understanding of this phenomenon.

2. Sferic Waveform Analysis

In their study, Rison et al. (2016) recorded sferics from NBEs using an FA and evaluated the sferic waveforms using a MTLE with height model, which was previously employed for return strokes by Nucci and Rachidi (1989) and Rachidi and Nucci (1990). Adopting the sign convention where a negative current moves positive charge downward (i.e., electrons flow upward), this transmission line scheme is sketched in Figure 1. A positive NBE current front propagates downward from an altitude H_2 to H_1 , with a channel length of $L = H_2 - H_1$. The downward current I_d (red curve in the figure) decreases exponentially along its propagation channel with an attenuation rate λ_d :

$$I_d(z, t) = I(t - (H_2 - z)/v_d) e^{-(H_2 - z)/\lambda_d}, \quad (1)$$

where v_d is the downward propagation velocity, related to the downward propagation time t_d by $v_d = L/t_d$. The injected current I_d has a double-exponential waveform

$$I(t) = \frac{I_0 e^{\alpha t}}{1 + e^{(\alpha + \beta)t}} \quad (2)$$

where $\alpha = 1/\tau_1$, $\beta = 1/\tau_2$ are the rise and fall time constants. The amplitude I_0 can be normalized to the peak current I_{peak} by setting

$$I_0 = I_{peak} \left(1 + \frac{\alpha}{\beta}\right) \left(\frac{\alpha}{\beta}\right)^{\left(\frac{-\alpha}{\alpha + \beta}\right)}. \quad (3)$$

Let us focus on the events NBE1 and NBE3 analyzed by Rison et al. (2016) and initially assume that the current dies out as it reaches the end of the channel at H_1 . In the following, we adopt the same geometry as Rison et al. (2016), derived from their observations. This includes the observation distance ρ , maximum channel altitude H_2 , channel length L and the velocity v listed in Table 1 for the case NBE1 and NBE3, respectively.

We compute the electric field at ground level at a location that follows the source-observer geometry of the events (see Table 1) by employing two approaches: Uman's equation (Uman et al., 1975) and a solution of the complete Maxwell's equations using the Finite-Difference Time-Domain (FDTD) method (Li et al., 2020). We use Uman's equation with the same current parameters used by Rison et al. (2016). The adopted parameters are listed in

Table 1*The Parameters of the NBE-Producing Current Used in the Simulation for Cases NBE1 and NBE3 Reported by Rison et al. (2016)*

		Parameters adopted in Rison et al. (2016)									
ID	Method	I_{peak} (kA)	τ_1 (μ s)	τ_2 (μ s)	λ (m)	ρ (km)	H_2 (m)	L (m)	v (m/s)		
NBE1	Uman's eq/Shao's eq with MTLE model	−55.2	0.8	6.0	900	5.5	6,000 ^a	455	3.5×10^7		
NBE3	Uman's eq/Shao's eq with MTLE model	−63.4	0.3	2.3	900	3.3	6,600	560	3.5×10^7		
ID	Method	Simulation-determined parameters ^b					Interferometer-determined parameters ^c				
		I_{peak} (kA)	τ_1 (μ s)	τ_2 (μ s)	λ_d (m)	λ_u (m)	ρ (km)	H_2 (m)	L (m)	t_d (μ s)	t_u (μ s)
NBE1	Uman's eq with rebounding MTLE model	−30.5	0.8	7.0	374.9	857.6	5.5	6,700	720	12	13
NBE3	Uman's eq with rebounding MTLE model	−61.7	0.3	3.4	378.7	113.7	3.3	6,600	412	11	6

Note. Three different models were used in simulation: Uman's equation (Uman et al., 1975) with the MTLE model, Shao's equation (Shao et al., 2004, 2005) with the MTLE model, and Uman's equation with the rebounding MTLE model.

^aThe altitude H_2 is derived from the LMA data, see Rison et al. (2016) for details. ^bThe current amplitude I_{peak} , rise and fall time constants (τ_1 , τ_2), as well as the downward and upward exponential attenuation rates (λ_d , λ_u) are best-fit parameters defining $I(z, t)$ to the spheric waveforms of NBE1 and NBE3. ^cThe observation distance ρ , altitude H_2 , length L , the downward and upward propagation times (t_d , t_u) are determined by the interferometer data in Rison et al. (2016) (see Figure 2).

table 1, and the current pulse as a function of height resulting from these parameters is shown in Figure S1 in Supporting Information S1, panels (a) and (b), whereas Figure 3 contains the computational results (blue line and blue triangles), as well as the measured spheric observations (black line).

The two computational approaches agree with each other to very good accuracy but they differ from the measured waveforms. At around 17 μ s for NBE1 and, more markedly, at around 21 μ s for NBE3, the model predicts negative deviations that are conspicuously absent in the observations. These deviations result from a peak in the radiation component, proportional to the time-derivative of the current, emitted as the current terminates abruptly at the end of the channel. This peak has previously been referred to as the “mirror image” effect (Shoory et al., 2009; Uman et al., 1975).

In their work, Rison et al. (2016) used a different approach to compute the radiation field. Instead of Uman's equation, which is a particularization of the retarded time, integral formulation of Maxwell's equations (called Jefimenko's or Schott's equations [Zangwill, 2013, p. 726]; a more general version of Uman's equation valid for arbitrary time-dependent current density can be found in Shao (2016)), they applied Shao's expression (Shao et al., 2005, equation 11), which disregards the current discontinuity at the end of the TL and applies only to cases where the current is sufficiently attenuated before it reaches that point. This approach produces the green curves in panels (a) and (b) of Figure 3. The late radiative peak is absent and the calculations agree reasonably well with the observations.

This raises the question of why reproducing the observations requires suppressing the radiative peak. We considered the possibility that the current does not disappear abruptly at the end of the TL but instead vanishes gradually, damping the radiation peak below the instrument's sensitivity. To investigate this, we extended the MTLE model with an extra region where the current decays smoothly but we found that an unrealistically long extension with $d \geq 5$ km is required to sufficiently attenuate the radiative peaks (see Figure S3 and accompanying text in Supporting Information S1 for further details).

On the basis of the idea of the bouncing-wave proposed by Nag and Rakov (2010a) and the rebounding fast breakdown waves discussed by Attanasio et al. (2021), we assume that the current, instead of vanishing, reverses direction and heads upward when it reaches the end of the TL channel. This eliminates the current discontinuity at the end of the channel. Besides, the existence of an upward-directed pulse is supported by the interferometer traces observed by Rison et al. (2016) (see Figures 2a and 2b in Rison et al. (2016) for details). The uncertainties of the elevation and azimuth source locations measured by the high-speed broadband VHF interferometer are presented in supplementary figures 15–17 in Rison et al. (2016).

One difference of the proposed model with the one proposed by Nag and Rakov (2010a) is that, to ensure the current continuity, we prescribe that the current is attenuated as it propagates, instead of having a discrete attenuation factor at the ends of the TL. Because of this difference and because we assume only one direction

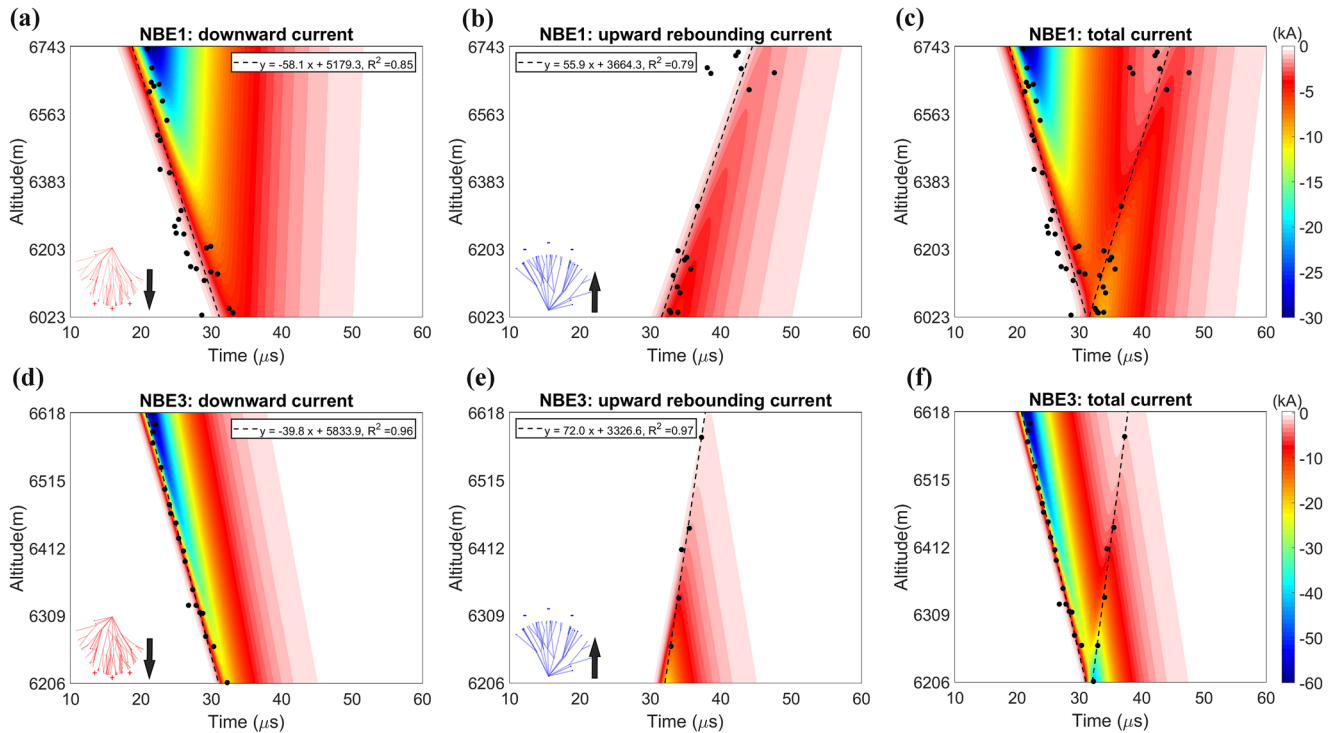


Figure 2. The current distribution of rebounding MTLE model for NBE1 and NBE3 along with the interferometer data observed by Rison et al. (2016). NBE1 and NBE3: (a), (d) downward current I_d (positive streamer propagates downward), (b), (e) upward rebounding current I_u (negative streamer propagates upward) and (c), (f) total current I_t . Note that the time of interferometer data here has been corrected to the source time. The detailed interferometer data can be found in Rison et al. (2016).

reversal, we refer to our model as “rebounding wave” although it could also arguably be called “modified bouncing wave.”

In our model, we include this upward rebounding current I_u (marked as a blue curve in Figure 1) as a pulse with a velocity v_u along the previous path and also following the MTLE model but with a different attenuation rate λ_u :

$$I_u(z, t) = I(t - L/v_d - (z - H_1)/v_u) e^{-L/\lambda_d} e^{-(z-H_1)/\lambda_u}, \quad (4)$$

where t_u is the upward propagation time related to the upward velocity by $v_u = L/t_u$ and the factor e^{-L/λ_d} ensures the continuity between the downward and the upward-propagating pulses.

The total current I_t is the sum of the downward current I_d and the upward rebounding current I_u :

$$I_t(z, t) = I_d(z, t) + I_u(z, t). \quad (5)$$

As shown in Figure 2, the downward and upward propagation time (t_d and t_u) are obtained by fitting the interferometer traces for both NBE1 and NBE3 with the best-fit lines shown in panels (a,b) for NBE1 and panels (d,e) for NBE3. We fit the parameters defining the current $I(z, t)$ to the sferic waveforms of NBE1 and NBE3, with the best-fit results listed in Table 1. The downward, upward and total current as a function of height for the rebounding MTLE model are represented in Figure 2 along with the interferometer data, panels (a–c) for NBE1 and (d–f) for NBE3. In all cases discussed here, the upward current pulse is attenuated to a negligible value before it reaches the upper top boundary. The resulting waveforms derived from Uman's equation with the rebounding MTLE model and the FDTD model are plotted with a red line and red triangles in panels (a) and (b) of Figure 3. Panels (c) and (d) of that figure show the three components of the electric field resulting from Uman's equation using both the MTLE model and the rebounding MTLE model. The late radiation peak is almost completely suppressed and the model predictions match the observations with the same accuracy as Shao's equation. It is shown that the rebounding currents propagate upward following the previous path, which agrees with the interferometer traces for both NBE1 and NBE3. Note that for NBE1 the absence of the radiation peak can also be explained by a strong attenuation of the downward current; with the parameters of Table 1 the sferic is weakly sensitive to the

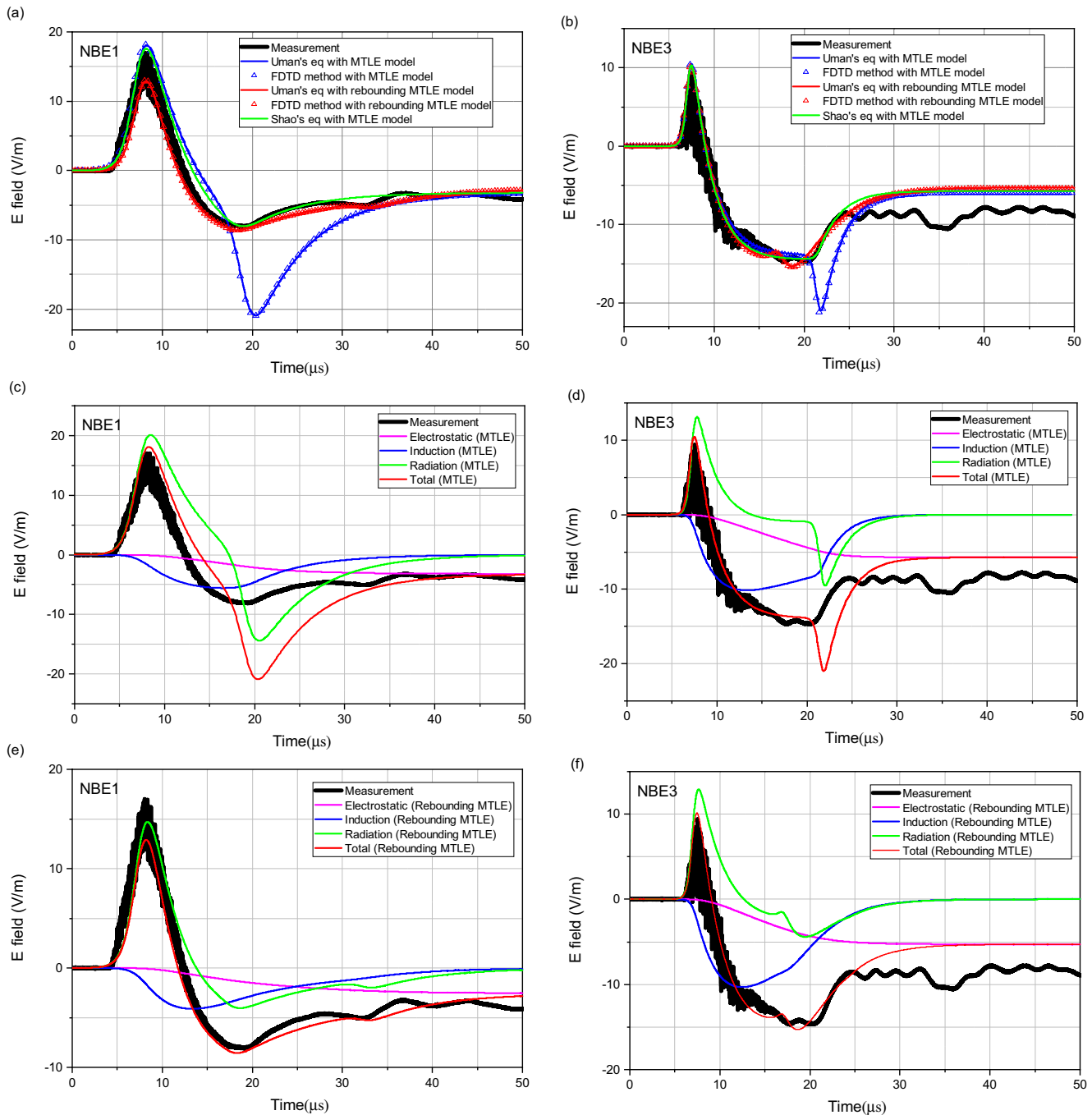


Figure 3. Comparison between simulation and measurement corresponding to the case NBE1 (a, c, e) and NBE3 (b, d, f) in Rison et al. (2016). (a), (b) Different approaches: Uman's equation (Uman et al., 1975) and full-wave FDTD method with the MTLE model, Uman's equation and full-wave FDTD method with the rebounding MTLE model, and Shao's equation with the MTLE model. The electrostatic, induction and radiation components of the total electric field calculated by using Uman's equation with the MTLE model (c), (d) and the rebounding MTLE model (e), (f).

parameters of the upward current. This is not the case for NBE3, which cannot be reasonably explained without an upward current and therefore provides the strongest evidence for our conclusion.

Both Shao's expression and the rebounding MTLE model underestimate the electric field in the tail of the spheric waveform. As discussed by Rison et al. (2016), NBE3 is more complex than NBE1 and contains features such as

a small tilt and a substantial azimuthal spread (see figure 9 in the supplementary material of Rison et al. (2016)). This deserves further analysis but falls out of the scope of the present work.

3. Discussion and Conclusions

Our results show that the NBE sferics published by Rison et al. (2016) are better explained if one assumes that once the primary current pulse has propagated about 400–700 m, it triggers a counter-propagating current pulse. The data are best fit when downward and upward currents rebound continuously; otherwise, the predicted waveform partly recovers the radiation peak that is absent in the observations. This secondary pulse is also observed in the interferometer data reported by Rison et al. (2016); Tilles et al. (2019).

The results also indicate that the measured NBE sferics are consistent with a current distribution with a significant spatial extent where FPB and FNB overlap within a significative volume. Although one cannot exclude the possibility that other current distributions may also reproduce the sferics, we believe that the existence of a secondary fast breakdown current is a plausible explanation for the absence of the radiation peak to better agree with the observations.

In their original bouncing-wave model, Nag and Rakov (2010a) explained the secondary pulse as the reflection of a wave as it reaches the channel ends. The simulated results by using the bouncing-wave model based on “Uman's equation with the MTLE model” along with the parameters shown in Table 1 as well as adopting different sets of values for the current reflection coefficients are discussed in the Supplemental Materials which do not match well with the measurements (see Figures S4 and S5, and the text there in Supporting Information S1). In addition, we further compared the results of the rebounding MTLE model with the well-known two-station measurements reported by Eack (2004). The simulations agree well with the measurements for both near and far stations (see Figure S6 and Table S1 in Supporting Information S1). Note that, in the rebounding MTLE model, the downward and upward propagation times (t_d and t_u) are determined by the modeling since there is no available interferometer observation. Assuming a downward attenuation rate $\lambda_d = 1 \times 10^5$ m and an upward attenuation rate $\lambda_u = 100$ m, the results corresponding to the rebounding MTLE model are found to be similar to those calculated by the bouncing-wave model in Nag and Rakov (2010a).

On the other hand, the interferometer observations suggest that both the downward and upward pulses share the same nature, most likely being systems of streamers as discussed by Attanasio et al. (2021). The triggering of streamer channels by streamers of opposite polarity is not uncommon. Kochkin et al. (2012) captured images where a positive streamer corona triggers negative streamers as it approaches an electrode. The same group found positive streamers emerging from the channels of preceding negative streamers (Kochkin et al., 2014) and a similar process explains the shape of carrot sprites in the upper atmosphere (Malagón-Romero et al., 2020). In the numerical simulations of Malagón-Romero et al. (2020), similar currents flow through the channels of the downward and upward streamers because they are connected through electrically conducting regions.

We also note that collisions between streamers of opposite polarities have been proposed as a source of X-rays and as precursors of Terrestrial Gamma-ray Flashes (TGF; Babich & Bochkov, 2017; Cooray et al., 2009; Ihaddadene & Celestin, 2015; Köhn et al., 2017; Luque, 2017). Tilles et al. (2020) presented a case where alternating fast positive and negative breakdown precedes a large current pulse (EIP) which is likely associated with a TGF (Pu et al., 2019). Note that the rebounding-wave model proposed here is different from the physical picture described by Huang et al. (2021): in the cases that they analyzed, negative and positive fast breakdowns appeared to be simultaneously launched from the same region.

A final conclusion concerns the persistence of electric fields after the fast breakdown discharges. That a secondary discharge is allowed to propagate suggests an incomplete screening of the electric field. Furthermore, the alternating fast positive and negative breakdown reported by Tilles et al. (2020) hints at the possibility of very weak screening of the electric fields, a conclusion that is relevant to estimates of the driving field as analyzed by Cummer (2020) and has key implications for physical models of fast breakdown.

Data Availability Statement

Open Research All the data for generating the figures are available at <https://doi.org/10.5281/zenodo.5960528>.

Acknowledgments

The authors would like to thank Dr. Xuan-Min Shao for his helpful advice and comments during the preparation of this manuscript. This work was supported by the European Research Council (ERC) under the European Union H2020 programme/ERC grant agreement 681257. Additionally, this work was supported by the Spanish Ministry of Science and Innovation, MINECO, under project PID2019-109269RB-C43 and FEDER program. Dongshuai Li, Alejandro Luque, and F. J. Gordillo-Vázquez acknowledge financial support from the State Agency for Research of the Spanish MCIU through the "Center of Excellence Severo Ochoa" award for the Instituto de Astrofísica de Andalucía (SEV-2017-0709).

References

- Attanasio, A., Da Silva, C. L., & Krehbiel, P. R. (2021). Electrostatic conditions that produce fast breakdown in thunderstorms. *Journal of Geophysical Research: Atmospheres*, 17. <https://doi.org/10.1029/2021JD034829>
- Attanasio, A., Krehbiel, P. R., & Da Silva, C. L. (2019). Griffiths and Phelps lightning initiation model, revisited. *Journal of Geophysical Research: Atmospheres*, 124(14), 8076–8094. <https://doi.org/10.1029/2019JD030399>
- Babich, L., & Bochkov, E. (2017). Numerical simulation of electric field enhancement at the contact of positive and negative streamers in relation to the problem of runaway electron generation in lightning and in long laboratory sparks. *Journal of Physics D*, 50(45), 455202. <https://doi.org/10.1088/1361-6463/aa88fd>
- Cooray, V., Arevalo, L., Rahman, M., Dwyer, J., & Rassoul, H. (2009). On the possible origin of X-rays in long laboratory sparks. *Journal of Atmospheric and Solar-Terrestrial Physics*, 71(17–18), 1890–1898. <https://doi.org/10.1016/j.jastp.2009.07.010>
- Cooray, V., Cooray, G., Rubinstein, M., & Rachidi, F. (2020). Modeling compact intracloud discharge (CID) as a streamer burst. *Atmosphere*, 11(5), 549. <https://doi.org/10.3390/atmos11050549>
- Cummer, S. A. (2020). Indirectly measured ambient electric fields for lightning initiation in fast breakdown regions. *Geophysical Research Letters*, 47(4), e86089. <https://doi.org/10.1029/2019GL086089>
- Da Silva, C. L., & Pasko, V. P. (2015). Physical mechanism of initial breakdown pulses and narrow bipolar events in lightning discharges. *Journal of Geophysical Research: Atmospheres*, 120(10), 4989–5009. <https://doi.org/10.1002/2015JD023209>
- Eack, K. B. (2004). Electrical characteristics of narrow bipolar events. *Geophysical Research Letters*, 31(20). <https://doi.org/10.1029/2004GL021117>
- Griffiths, R. F., & Phelps, C. T. (1976). A model for lightning initiation arising from positive corona streamer development. *Journal of Geophysical Research*, 81(21), 3671–3676. <https://doi.org/10.1029/JC081i021p03671>
- Gurevich, A., Zybin, K., & Roussel-Dupre, R. (1999). Lightning initiation by simultaneous effect of runaway breakdown and cosmic ray showers. *Physics Letters A*, 254(1), 79–87. [https://doi.org/10.1016/S0375-9601\(99\)00091-2](https://doi.org/10.1016/S0375-9601(99)00091-2)
- Gurevich, A., & Zybin, K. P. (2001). Runaway breakdown and electric discharges in thunderstorms. *Physics-Uspekhi*, 44(11), 1119–1140. <https://doi.org/10.1070/pu2001v044n11abeh000939>
- Hamlin, T., Light, T. E., Shao, X. M., Eack, K. B., & Harlin, J. D. (2007). Estimating lightning channel characteristics of positive narrow bipolar events using intrachannel current reflection signatures. *Journal of Geophysical Research: Atmospheres*, 112(D14), 108. <https://doi.org/10.1029/2007JD008471>
- Huang, A., Cummer, S. A., & Pu, Y. (2021). Lightning Initiation from fast negative breakdown is led by positive polarity dominated streamers. *Geophysical Research Letters*, 48, e2020GL091553. <https://doi.org/10.1029/2020GL091553>
- Ihaddadene, M. A., & Celestin, S. (2015). Increase of the electric field in head-on collisions between negative and positive streamers. *Geophysical Research Letters*, 42(13), 5644–5651. <https://doi.org/10.1002/2015GL064623>
- Karunarathne, S., Marshall, T. C., Stolzenburg, M., & Karunarathna, N. (2014). Modeling initial breakdown pulses of CG lightning flashes. *Journal of Geophysical Research: Atmospheres*, 119(14), 9003–9019. <https://doi.org/10.1002/2014JD021553>
- Karunarathne, S., Marshall, T. C., Stolzenburg, M., & Karunarathna, N. (2016). Electrostatic field changes and durations of narrow bipolar events. *Journal of Geophysical Research: Atmospheres*, 121(17), 10161–10174. <https://doi.org/10.1002/2016JD024789>
- Kochkin, P. O., Nguyen, C. V., Van Deursen, A. P. J., & Ebert, U. (2012). Experimental study of hard X-rays emitted from metre-scale positive discharges in air. *Journal of Physics D: Applied Physics*, 45(42), 425202. <https://doi.org/10.1088/0022-3727/45/42/425202>
- Kochkin, P. O., Van Deursen, A. P. J., & Ebert, U. (2014). Experimental study of the spatio-temporal development of metre-scale negative discharge in air. *Journal of Physics D: Applied Physics*, 47(14), 145203. <https://doi.org/10.1088/0022-3727/47/14/145203>
- Köhn, C., Chanrion, O., & Neubert, T. (2017). Electron acceleration during streamer collisions in air. *Geophysical Research Letters*, 44(5), 2604–2613. <https://doi.org/10.1002/2016GL072216>
- Kostinskiy, A. Y., Marshall, T. C., & Stolzenburg, M. (2020). The mechanism of the origin and development of lightning from initiating event to initial breakdown pulses (v.2). *Journal of Geophysical Research: Atmospheres*, 125(22), e2020JD033191. <https://doi.org/10.1029/2020JD033191>
- Leal, A. F., Rakov, V. A., & Rocha, B. R. (2019). Compact intracloud discharges: New classification of field waveforms and identification by lightning locating systems. *Electric Power Systems Research*, 173, 251–262. <https://doi.org/10.1016/j.epsr.2019.04.016>
- Le Vine, D. M. (1980). Sources of the strongest RF radiation from lightning. *Journal of Geophysical Research: Oceans*, 85(C7), 4091–4095. <https://doi.org/10.1029/JC085iC07p04091>
- Li, D., Liu, F., Pérez-Invernón, F. J., Lu, G., Qin, Z., Zhu, B., & Luque, A. (2020). On the Accuracy of ray-theory methods to determine the altitudes of intracloud electric discharges and ionospheric reflections: Application to narrow bipolar events. *Journal of Geophysical Research: Atmospheres*, 125(9), e2019JD032099. <https://doi.org/10.1029/2019JD032099>
- Li, D., Luque, A., Gordillo-Vázquez, F. J., Liu, F., Lu, G., Neubert, T., et al. (2021). Blue flashes as counterparts to narrow bipolar events: The optical signal of shallow in-cloud discharges. *Journal of Geophysical Research: Atmospheres*, 126(13), e2021JD035013. <https://doi.org/10.1029/2021JD035013>
- Liu, N., Dwyer, J. R., Tilles, J. N., Stanley, M. A., Krehbiel, P. R., Rison, W., et al. (2019). Understanding the radio spectrum of thunderstorm narrow bipolar events. *Journal of Geophysical Research: Atmospheres*, 124(10), 10134–10153. <https://doi.org/10.1029/2019JD030439>
- Liu, N., Scholten, O., Dwyer, J. R., Hare, B., Sterpka, C. F., Tilles, J., & Lind, F. D. (2021). Implications of multiple corona bursts in lightning processes for radio frequency interferometer observations. *Earth and Space Science Open Archive*, 12. <https://doi.org/10.1002/essoar.10509275.1>
- López, J. A., Montanyà, J., Van der Velde, O., Romero, D., Gordillo-Vázquez, F. J., Pérez-Invernón, F. J., et al. (2022). Initiation of lightning flashes simultaneously observed from space and the ground: Narrow bipolar events. *Atmospheric Research*, 268, 105981. <https://doi.org/10.1016/j.atmosres.2021.105981>
- Luque, A. (2017). Radio frequency electromagnetic radiation from streamer collisions. *Journal of Geophysical Research: Atmospheres*, 122(19), 10497–10509. <https://doi.org/10.1002/2017JD027157>
- Luque, A., & Ebert, U. (2014). Growing discharge trees with self-consistent charge transport: The collective dynamics of streamers. *New Journal of Physics*, 16(1), 013039. <https://doi.org/10.1088/1367-2630/16/1/013039>
- Lyu, F., Cummer, S. A., Qin, Z., & Chen, M. (2019). Lightning initiation processes imaged with very high frequency broadband interferometry. *Journal of Geophysical Research: Atmospheres*, 124(6), 2994–3004. <https://doi.org/10.1029/2018JD029817>
- Malagón-Romero, A., Teunissen, J., Stenbaek-Nielsen, H. C., McHarg, M. G., Ebert, U., & Luque, A. (2020). On the emergence mechanism of carrot sprites. *Geophysical Research Letters*, 47(1), e85776. <https://doi.org/10.1029/2019GL085776>
- Marshall, T., Bandara, S., Karunarathne, N., Karunarathne, S., Kolmasova, I., Siedlecki, R., & Stolzenburg, M. (2019). A study of lightning flash initiation prior to the first initial breakdown pulse. *Atmospheric Research*, 217, 10–23. <https://doi.org/10.1016/j.atmosres.2018.10.013>

- Marshall, T., Stolzenburg, M., Karunarathna, N., & Karunarathne, S. (2014). Electromagnetic activity before initial breakdown pulses of lightning. *Journal of Geophysical Research: Atmospheres*, 119(22), 12558–12574. <https://doi.org/10.1002/2014JD022155>
- Nag, A., & Rakov, V. A. (2010a). Compact intracloud lightning discharges: 1. Mechanism of electromagnetic radiation and modeling. *Journal of Geophysical Research: Atmospheres*, 115(D20). <https://doi.org/10.1029/2010JD014235>
- Nag, A., & Rakov, V. A. (2010b). Compact intracloud lightning discharges: 2. Estimation of electrical parameters. *Journal of Geophysical Research: Atmospheres*, 115(D20). <https://doi.org/10.1029/2010JD014237>
- Nucci, C. A., & Rachidi, F. (1989). Experimental validation of a modification to the transmission line model for LEMP calculation. In *8th symposium and technical exhibition on electromagnetic compatibility, Zurich, Switzerland*.
- Petersen, D., Bailey, M., Hallett, J., & Beasley, W. (2015). Laboratory investigation of corona initiation by ice crystals and its importance to lightning. *Quarterly Journal of the Royal Meteorological Society*, 141(689), 1283–1293. <https://doi.org/10.1002/qj.2436>
- Petersen, D., Bailey, M., Hallett, J., & Beasley, W. H. (2006). Laboratory investigation of positive streamer discharges from simulated ice hydro-meteors. *Quarterly Journal of the Royal Meteorological Society*, 132(615), 263–273. <https://doi.org/10.1256/qj.05.32>
- PHELPS, C. (1974). Positive streamer system intensification and its possible role in lightning initiation. *Journal of Atmospheric and Terrestrial Physics*, 36(1), 103–111. [https://doi.org/10.1016/0021-9169\(74\)90070-1](https://doi.org/10.1016/0021-9169(74)90070-1)
- Pu, Y., Cummer, S. A., Lyu, F., Briggs, M., Mailyan, B., Stanbro, M., & Roberts, O. (2019). Low frequency radio pulses produced by terrestrial gamma-ray flashes. *Geophysical Research Letters*, 46(12), 6990–6997. <https://doi.org/10.1029/2019GL082743>
- Rachidi, F., & Nucci, C. (1990). On the master, Uman, Lin, Standler and the modified transmission line lightning return stroke current models. *Journal of Geophysical Research: Atmospheres*, 95(D12), 20389–20393. <https://doi.org/10.1029/JD095iD12p20389>
- Rison, W., Krehbiel, P. R., Stock, M. G., Edens, H. E., Shao, X.-M., Thomas, R. J., et al. (2016). Observations of narrow bipolar events reveal how lightning is initiated in thunderstorms. *Nature Communications*, 7, 10721. <https://doi.org/10.1038/ncomms10721>
- Shao, X.-M. (2016). Generalization of the lightning electromagnetic equations of Uman, McLain, and Krider based on Jefimenko equations. *Journal of Geophysical Research: Atmospheres*, 121(7), 3363–3371. <https://doi.org/10.1002/2015JD024717>
- Shao, X.-M., Fitzgerald, T. J., & Jacobson, A. R. (2005). Reply to comment by Rajeev Thottappillil and Vladimir A. Rakov on "Radio frequency radiation beam pattern of return strokes: A revisit to theoretical analysis". *Journal of Geophysical Research: Atmospheres*, 110(D24). <https://doi.org/10.1029/2005JD005889>
- Shao, X.-M., Jacobson, A. R., & Fitzgerald, T. J. (2004). Radio frequency radiation beam pattern of lightning return strokes: A revisit to theoretical analysis. *Journal of Geophysical Research: Atmospheres*, 109(D19). <https://doi.org/10.1029/2004JD004612>
- Shao, X.-M., Lay, E., & Jacobson, A. R. (2012). On the behavior of return stroke current and the remotely detected electric field change waveform. *Journal of Geophysical Research: Atmospheres*, 117(D7). <https://doi.org/10.1029/2011JD017210>
- Shoory, A., Rachidi, F., Rubinstein, M., Moini, R., & Sadeghi, S. H. H. (2009). Why do some lightning return stroke models not reproduce the far-field zero crossing? *Journal of Geophysical Research: Atmospheres*, 114(D16). <https://doi.org/10.1029/2008JD011547>
- Smith, D. A., Eack, K. B., Harlin, J., Heavner, M. J., Jacobson, A. R., Massey, R. S., & Wiens, K. C. (2002). The Los Alamos Sferic array: A research tool for lightning investigations. *Journal of Geophysical Research: Atmospheres*, 107(D13). ACL 5-1–ACL 5-14. <https://doi.org/10.1029/2001JD000502>
- Smith, D. A., Heavner, M. J., Jacobson, A. R., Shao, X. M., Massey, R. S., Sheldon, R. J., & Wiens, K. C. (2004). A method for determining intracloud lightning and ionospheric heights from VLF/LF electric field records. *Radio Science*, 39(1), RS1010. <https://doi.org/10.1029/2002RS002790>
- Smith, D. A., Shao, X. M., Holden, D. N., Rhodes, C. T., Brook, M., Krehbiel, P. R., et al. (1999). A distinct class of isolated intracloud lightning discharges and their associated radio emissions. *Journal of Geophysical Research: Atmospheres*, 104(D4), 4189–4212. <https://doi.org/10.1029/1998JD00045>
- Soler, S., Pérez-Invernón, F. J., Gordillo-Vázquez, F. J., Luque, A., Li, D., Malagón-Romero, A., et al. (2020). Blue optical observations of narrow bipolar events by ASIM suggest corona streamer activity in thunderstorms. *Journal of Geophysical Research: Atmospheres*, 125(16), e2020JD032708. <https://doi.org/10.1029/2020JD032708>
- Stock, M. G., Akita, M., Krehbiel, P. R., Rison, W., Edens, H. E., Kawasaki, Z., & Stanley, M. A. (2014). Continuous broadband digital interferometry of lightning using a generalized cross-correlation algorithm. *Journal of Geophysical Research: Atmospheres*, 119(6), 3134–3165. <https://doi.org/10.1002/2013JD020217>
- Stolzenburg, M., Marshall, T. C., Bandara, S., Hurley, B., & Siedlecki, R. (2021). Ultra-high speed video observations of intracloud lightning flash initiation. *Meteorology and Atmospheric Physics*, 133(4), 1177–1202. <https://doi.org/10.1007/s00703-021-00803-3>
- Stolzenburg, M., Marshall, T. C., Karunarathne, S., Karunarathna, N., Vickers, L. E., Warner, T. A., et al. (2013). Luminosity of initial breakdown in lightning. *Journal of Geophysical Research: Atmospheres*, 118(7), 2918–2937. <https://doi.org/10.1002/jgrd.50276>
- Tilles, J. N., Krehbiel, P. R., Stanley, M. A., Rison, W., Liu, N., Lyu, F., et al. (2020). Radio interferometer observations of an energetic in-cloud pulse reveal large currents generated by relativistic discharges. *Journal of Geophysical Research: Atmospheres*, 125(20), e2020JD032603. <https://doi.org/10.1029/2020JD032603>
- Tilles, J. N., Liu, N., Stanley, M. A., Krehbiel, P. R., Rison, W., Stock, M. G., et al. (2019). Fast negative breakdown in thunderstorms. *Nature Communications*, 10(1), 1648. <https://doi.org/10.1038/s41467-019-09621-z>
- Uman, M. A., McLain, D. K., & Krider, E. P. (1975). The electromagnetic radiation from a finite antenna. *American Journal of Physics*, 43(1), 33–38. <https://doi.org/10.1119/1.10027>
- Watson, S. S., & Marshall, T. C. (2007). Current propagation model for a narrow bipolar pulse. *Geophysical Research Letters*, 34(4). <https://doi.org/10.1029/2006GL027426>
- Willett, J. C., Bailey, J. C., & Krider, E. P. (1989). A class of unusual lightning electric field waveforms with very strong high-frequency radiation. *Journal of Geophysical Research: Atmospheres*, 94(D13), 16255–16267. <https://doi.org/10.1029/JD094iD13p16255>
- Wu, T., Yoshida, S., Ushio, T., Kawasaki, Z., & Wang, D. (2014). Lightning-initiator type of narrow bipolar events and their subsequent pulse trains. *Journal of Geophysical Research: Atmospheres*, 119(12), 7425–7438. <https://doi.org/10.1002/2014JD021842>
- Zangwill, A. (2013). *Modern electrodynamics*. Cambridge University Press. <https://doi.org/10.1017/CBO9781139034777>